JOURNAL OF BACTERIOLOGY, Sept. 1986, p. 960–967
0021-9193/86/090960-08$02.00/0

Vol. 167, No. 3

Autoradiographic Studies of the Synthesis of RNA and Protein as a Function of Cell Volume in *Streptococcus faecium*

MICHAEL L. HIGGINS,[1]* ARTHUR L. KOCH,[2] DAVID T. DICKER,[1] AND LOLITA DANEO-MOORE[1]

Department of Microbiology and Immunology, Temple University School of Medicine, Philadelphia, Pennsylvania 19140,[1] and Department of Biology, Indiana University, Bloomington, Indiana 47405[2]

Received 4 October 1985/Accepted 9 June 1986

Mid-exponential-phase cultures were either labeled continuously with tritiated leucine and uracil or pulse-labeled with tritiated leucine. The amount of leucine and uracil incorporated into protein or RNA per cell was determined by grain counts of autoradiographs of cells seen in electron micrographs; the volume of each cell was determined by three-dimensional reconstruction. The average number of autoradiographic grains around cells continuously labeled with uracil and leucine increased linearly with cell volume. In contrast, while the average grain count around cells pulse-labeled with leucine increased in a near-linear fashion over most of the volume classes, less than the expected number of grains were seen around cells in large- and small-size classes. The distribution of grains around cells from both the continuously and pulse-labeled populations could be fit at the 5% confidence level with a Poisson distribution modified to take into consideration the volume distribution of each population of cells analyzed. These findings suggested that large changes in the density of RNA and protein do not occur in most cells as they increase in size; however, there may be decreases in the rate of protein synthesis in some large and small cells. The decrease in the rate of protein synthesis appears consistent with the hypothesis that new sites of envelope growth must be introduced into cells that are close to the division event to restore rapid growth.

We used high-resolution electron microscopic autoradiographic techniques combined with three-dimensional cell reconstruction methodology to determine the amount of radioactive leucine and uracil incorporated per unit volume in whole cells of *Streptococcus faecium*. This technology was used to ask the question how cellular protein and RNA content and rate of protein synthesis correlate during the cell cycle with cell volume. Not only is this question of general interest, but it is of special interest in considering various models of envelope growth for this organism.

It is well known that the streptococcal surface is assembled at discrete sites which can be identified on electron micrographs (11, 12). Each site assembles a cross wall. As a constricting division furrow bilaterally splits this cross wall, the two cleaved cross-wall layers separate and expand to form two new polar caps. The finished caps have a size invariant to the growth rate (5). Thus, as completion of new poles is approached, new sites must be initiated for the cell to continue to grow. On geometric grounds it is evident that as the division furrow constricts, more and more externalized cell wall surface is required to house each incremental increase in cell volume. Taking this into consideration, it has been hypothesized that in the terminal stages of growth-site development new sites are initiated because the increase in the volume of the existing growth site is not rapid enough to contain the cytoplasmic mass that is being synthesized (16). This might explain the fluctuations in cytoplasmic density seen by Mitchison (21) by interference light microscopy of cells of *S. faecium* growing in slide culture. Thus, in this view, new sites would form owing to an increase in cytoplasmic pressure resulting from a discontinuity between the growth in cell volume and mass.

In several previous investigations, autoradiography has been used to study the partitioning of cytoplasmic macromolecules between daughter bacteria. Van Tubergen and Setlow (29) presented evidence to suggest that radioactively labeled protein and RNA were evenly distributed among cells of *Escherichia coli*. Furthermore, Caro (1) and Caro and Forro (2) were able to show that the distribution of grains in the emulsion overlying sections of *E. coli* previously labeled with tritiated leucine or uracil fit a modified Poisson distribution that took into consideration the distribution of the sizes of the cross sections analyzed. Finally, Ecker and Kokaisl (4) showed that the number of grains around cells of *Salmonella typhimurium* labeled with radioactive protein or RNA precursors increased in direct proportion with cell length as measured with a light microscope. These authors went on to equate increases in length with cell size. However, it should be noted that the calculation of cell volume from length measurements by light microscopy is open to considerable error. Thus, to our knowledge no study exists in which the relationship of cell mass (as determined by autoradiographic grain distribution around cells with radioactively labeled protein or RNA) to cell volume has been rigorously established. We approached this question in two ways. First, we examined directly whether the mean grain count of a subset of cells of a narrow volume range was directly proportional to volume, and second, we used an approach similar to Caro's (1) by assuming that a population of cells uniformly labeled with radioactive precursors of protein or RNA should best fit a modified Poisson function which reflects the distribution of cell sizes. It is difficult for us to compare our work with that of Caro, in that he did not give the details of his fitting procedure. Our fitting approach is based on computer modeling involving a very large number of computations and should be applicable to any bacterial population.

* Corresponding author.

MATERIALS AND METHODS

Cell growth. Cells of *S. faecium* ATCC 9790 were grown at 37°C as described previously (13) in a chemically defined medium (25) in which the L-tryptophan concentration was lowered to 20 μg/ml to eliminate chains (27). The mass doubling time (T_D) of cultures was between 82 and 90 min and was increased from about 30 min by reducing the glutamic acid concentration of the medium from 300 to 20 μg/ml in the absence of glutamine (28). Under these conditions cells grew exponentially but with an increased doubling time.

Before being used for study, cultures were required to undergo 12 doublings in mass. For continuous-labeling conditions, radioactive leucine or uracil was present in the medium throughout all 12 mass doublings. The day before cells were needed, a tube containing defined medium with or wihtout radioactive precursors was inoculated to bring the initial concentration to ca. 5×10^6 cells per ml. The culture was allowed to undergo six mass doublings in the exponential phase of growth. At this time, the culture was used to inoculate a quantity of chilled (ca. 5°C) medium in a flask. Again, the initial concentration was adjusted to ca. 5×10^6 cells per ml. The flask was then placed in a water bath filled with ice and was housed in a cold room. A timer was used to turn on the water bath at an appropriate time during the evening so that by morning the culture had undergone about four mass doublings at 37°C. When the culture achieved six mass doublings, it was either harvested or pulse-labeled, chased, and then harvested.

For continuous-labeling conditions, high-specific-activity L-[4,5-^{3}H]leucine (New England Nuclear Corp., Boston, Mass.) or [5,6-^{3}H]uracil (Amersham Corp., Arlington Heights, Ill.) was added to a final concentration of 20 or 1.3 μCi/ml, respectively, in medium which contained in the respective cases either 15 or 20 μg of unlabeled leucine or uracil per ml. For the pulse-chase experiments, 10 μCi of L-[4,5-^{3}H]leucine was added to the culture containing 15 μg of nonradioactive leucine per ml. After 5 min, the label was chased for 3 min by the addition of 1,000 times the concentration of nonradioactive leucine before fixation. Under continuous-labeling conditions 100% of the leucine within the cells was in cold-5% perchloric acid-precipitable material, and 68% of this label was in hot-perchloric acid-precipitable material (e.g., protein). During the formaldehyde treatment for fixation of cells there was a loss of 12% of labeled leucine, and none of this loss was from the hot-perchloric acid precipitable counts. Thus, formaldehyde-fixed cells contained a high proportion (86%) of their radioactivity in protein. In the pulse-labeled, formaldehyde-treated cells, 83% of the labeled leucine was in protein. There was a 13% loss of acid-precipitable labeled uracil in formaldehyde-fixed cells, and over 92% of the counts were in alkali-sensitive, RNase-sensitive material. Thus, little of the radioactivity was transferred into DNA or other cellular components. The data presented for each labeling condition represent a single experiment.

Electron microscopy. Cells were fixed by the addition to cultures of formaldehyde (prepared from paraformaldehyde) to a final concentration of 8.33% (7). After fixation, cells were washed four times in distilled water and resuspended in water to ca. 5×10^{10} cells per ml. Drops of this cell suspension were placed on carbon-stabilized Formvar films that had been mounted on copper grids (400 by 100 mesh). Just before use, the films were treated with a solution of 0.1% polylysine made in water and were then washed in a stream of water. Cells adhering to the Formvar films were dehydrated in ethanol, dried by the critical-point method, and coated with carbon in a Balzers high-vacuum unit (model BA-360M; Balzers, Liechtenstein). Grids containing and not containing cells were then coated in the dark with undiluted Nuclear Research Emulsion L4 (Ilford, Ltd., Basildon, Essex, England) by either the dipping (19) or the wire loop (6) method.

The wire loop procedure produced the most even distribution of silver grains, and it was used in all experiments reported here. To establish the variability in emulsion thickness, grids exposed to light and not containing cells were examined before and after development. The evenness of the distributrion of grains was established as a part of each experiment. If the grain distribution was even, a new set of grids was prepared. Grids were stored over silica gel in a horizontal position at 4°C between 15 and 83 days. At the end of the exposure time, the emulsions were processed in fine-grain developer by the gold latentsification procedure described by Kowpriwa (20). After air drying, grids were examined in a Hitachi H-600 electron microscope at an instrumental magnification of ×20,000. For a given specimen, each row of grid bar openings was studied, sequentially moving from left to right and top to bottom of the field of view. All unclumped cells within a given grid bar opening were photographed without selection. Cells were photographed on 35-mm film (Technical Pan, 2415; Eastman Kodak Co., Rochester, N.Y.), using a mixed secondary and transmission scanning electron image. Secondary electrons afforded surface information, while the transmission signal allowed silver grains to be differentiated from cellular material on the basis of the higher density of the silver grains. To speed up photography, a 5-s scan image was used. While the 5-s image resulted in a decrease in resolution in comparison to the slower 120-s photoscan image normally used for photography, the 5-s scan image appeared to be more than adequate for three-dimensional reconstruction of the cell surface, and the time savings more than compensated for the loss of resolution.

Three-dimensional reconstructions of cells were performed by converting the cell perimeter seen in electron micrographs into a series of x,y coordinates by tracing these perimeters with an electronic digitizer (model EGC; Numonics Corp., North Wales, Pa.). The coordinates were mathematically rotated around the longitudinal axis of the cell by using a computer (model 4051; Tektronix, Inc., Beaverton, Ore.) to estimate the volume of each cell and its components (7, 10). Please note that because these cells have been fixed and dehydrated the volumes obtained by this procedure are the relaxed volumes of the cells studied. These volume measurements, plus the number of grains observed over each cell and in an area of 0.5 μm around the cell perimeter, the number of grains observed outside this perimeter (background grains) in each film frame, and the grid bar opening identification number, were recorded on magnetic tape. In some grids, a few areas were found where the background counts were excessively high or low. In this case all cells photographed in this grid bar opening were excluded from analysis. Owing to slight differences in efficiency between coated grids, Poisson distributions were fitted to data from cells gathered from a single grid. These same cells were used to study the relationship between average grain count and cell volume (see Fig. 1). However, to study this relationship for the cells pulse-labeled with leucine (see Fig. 1C), we added cells from a second grid coated at the same time on which the difference between average grain counts was less

than 0.7 grains per cell. These populations were pooled to increase the numbers of cells for quantitation in the large- and small-volume classes in which an accurate assessment of grain count became quite important in this investigation. The density of background grains on any portion of a specimen was estimated by determining the average number of grains per unit area located 0.5 μm from any cell perimeter as seen in photographic films taken from any given grid bar opening. The correction for the number of cells minus background counts when used was carried out by (i) multiplying the projected area of a cell analyzed by the mean number of background counts per square micrometer as determined for the grid bar opening in question, (ii) subtracting the resulting number of grains owing to background from the number of grains counted for this cell, and (iii) rounding the corrected grain count to the nearest integer.

Computer program developed to produce volume-adjusted Poisson distributions. If all cells in a population of autoradiographs had the same amount of radioactivity, the distribution of grains over cells should follow a Poisson function:

$$P(n) = m^n e^{-m}/n! \quad (1)$$

where n is the number of grains around a cell, m is the mean number of grains per cell, and $P(n)$ is the fraction of the population predicted to have a given number of grains. This distribution can be transformed into a straight-line function in n as described by Hanawalt et al. (8):

$$H(n) = \ln [P(n)n!] = n \ln m - m \quad (2)$$

On the assumption that the cell content of protein and RNA and the rate of synthesis of these substances is proportional to cell volume, equation 1 was applied in a modified way. In this assumption, the distribution of grains should reflect the observed variation in cell size of the population of cells (e.g., see Fig. 1). For each cell size class of such a population, the Poisson function applies in the form:

$$P_i(n) = (FV_i)^n e^{-FV_i}/n! \quad (3)$$

where V_i is the average volume of each class of cells and F is the single adjustable parameter used in fitting an actual set of data points. F is the radioactivity per unit volume of cytoplasm. Thus, the modification simply assumes that the radioactivitiy in a cell is proportional to its volume (V_i in equation 3). The cells were grouped in volume classes which each spanned an increment of 0.5 μm^3. The volume used for V_i was the midpoint of the volume interval. A program was developed to use equation 3 repetitively to calculate the expected fraction of cells observed in each volume class that would have a given number of grains. In this procedure, initially equation 3 is used to calculate the frequency of cells in the smallest volume class, which would have zero grains (using an initial value for F tested by the experimenter). This frequency, once calculated, must be scaled to reflect the relative frequency of cells actually seen experimentally in this size range. This is done simply by multiplying the output of equation 3 by the actual frequency of cells seen in the volume class observed. This process is repeated until the frequency of cells with zero grains has been calculated for all observed volume classes. The sum of all these scaled frequencies represents the expected frequency of all the cells in the total population that would have zero grains for a given value of F. Then this process is carried out again for $n = 1$, etc., until the expected frequencies of cells with all the observed numbers of grains have been calculated, to calculate the volume-adjusted distribution for the particular value of F. Then the entire procedure is repeated with different values of F to find that distribution affording a best fit to the experimental data. The criterion for goodness of fit of the calculated frequencies as compared with the actual frequencies was the minimization of the D_{max} parameter of the Kolmolgorov-Smirnov procedure (26). The best-fitting distribution is referred to in the remainder of this text as a volume-adjusted Poisson. Values of F yielding the best fit were 35.65, 67.4, and 12.33, respectively, for Fig. 2B, 2D, and 2F.

RESULTS AND DISCUSSION

RNA, protein content, and rate of synthesis as a function of cell volume. In cells continuously labeled for many generations with either tritiated uracil or leucine, the average number of autoradiographic grains around exponential-phase cells of *S. faecium* increased linearly with cell size until cell volumes exceeded about 0.375 μm^3 (Fig. 1A and B). At volumes greater than 0.375 μm^3, the increases in grain count became erratic, which in large part reflects the smaller numbers of cells that were available for quantitation in these large-volume classes. In contrast, when cells pulse-labeled with leucine were examined in the same manner (Fig. 1C), the cell volume range over which the average grain count increased in a linear fashion appeared to be smaller, about 0.15 to 0.325 μm^3, with larger and smaller cells showing a nonlinear relation with increasing cell size. The decrease in the averge grain count that occurred at the higher volumes in these pulse-labeled cells showed a relatively smooth decline (Fig. 1C). In contrast, no consistent decline was seen in the continuously labeled cells (Fig. 1A and B). Thus, the results obtained from the continuously labeled cells suggested that RNA and protein increased in a linear manner with cell volume, whereas the data from the pulse-labeled cells indicated that there might have been decreases in the rate of protein synthesis in very small and large cells.

To test whether the mass of the continuously and pulse-labeled cells increased proportionally to volume, we examined the pattern of grain distributions around these cells (Fig. 2A, C, and E). If the hypothesis was correct that for most cells the amount of radioactivity incorporated is proportional to cell size, then a simple Poisson distribution should not fit these grain distributions, for this would mean that all cells regardless of their size would have the same amount of radioactivity. However, a Poisson distribution modified to take into consideration the exact range of cell volumes observed in each population should fit the grain distributions. In our terminology, we refer to such modified distributions as volume-adjusted Poisson distributions. To assist the reader in visually assessing the degree to which normal and volume-adjusted Poisson distributions fit the data in Fig. 2A, C, and E, we used a plotting procedure developed by Hanawalt et al. (8). Here the logarithm of the frequencies of cells with a given number of grains multiplied by $n!$ is plotted for each population of cells studied (where n is the number of grains in a particular class). If the frequencies of grain distributions obeyed an ideal Poisson distribution, data points should fall on a straight line. The solid points shown in Fig. 2B, D, and F show that the data do not folow a normal Poisson distribution (the Poisson distribution fitted to each data set is shown by the dashed line) and that they more closely follow the volume-adjusted Poisson fitted to each population (the volume-adjusted Poisson is shown in each figure by the solid line). That the volume-adjusted Poisson

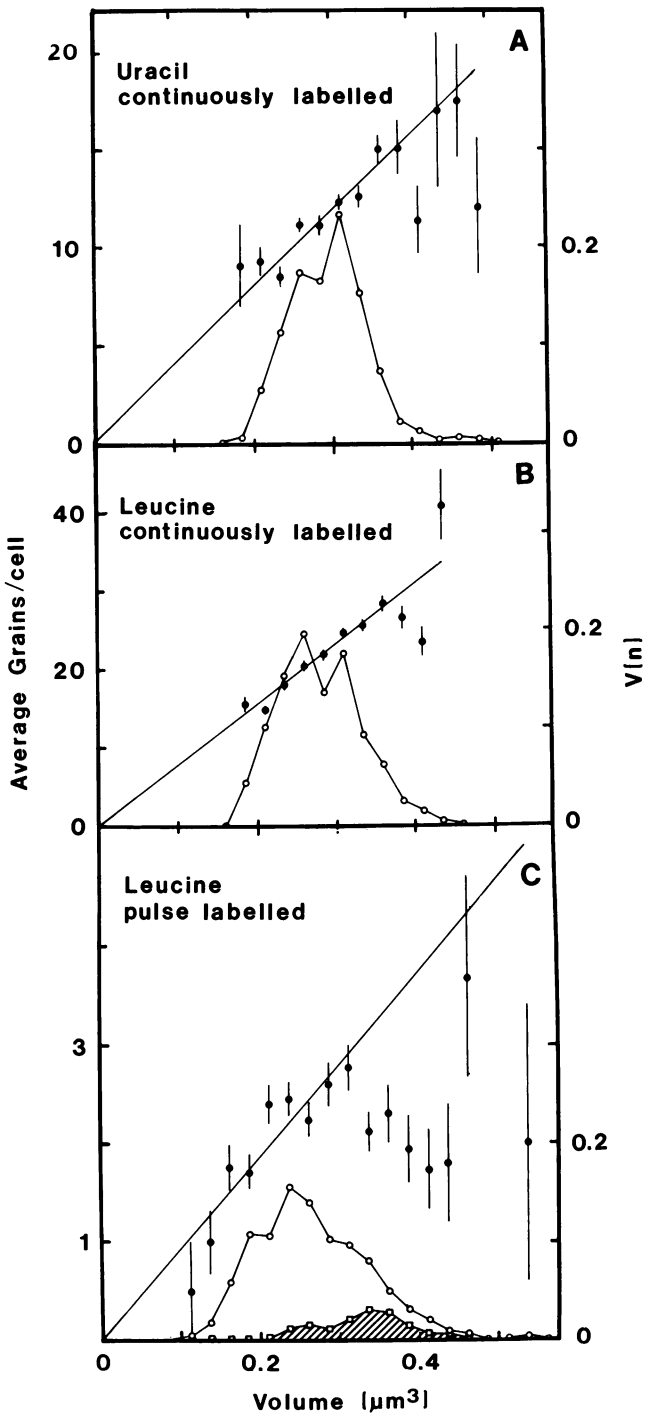

FIG. 1. Relation between average number of autoradiographic grains and cell volume (each class interval equals 0.025 μm^3). In each panel the solid points are the average number of grains per cell in the volume class. The error of measurement is shown above and below each point (± the mean × the square root of the number of cells analyzed). The open points give the frequency of cells found in each volume class, and the cross-hatched region of panel C shows the frequency of cells that have initiated new sites of envelope growth before division (Fig. 4, insert). (A) Data from cells continuously labeled with uracil; (B) data from cells continuously labeled with leucine; and (C) data from cells pulse-labeled with leucine for 5 min. In each case, the best line by eye was drawn through zero which would fit the greatest number of points. The number of cells analyzed for each experiment is the same as given in Table 1, except in panel C in which cells from a second grid were added to bring n to 545 to increase the number of cells that could be studied at high and low volumes.

TABLE 1. Goodness of fit of normal and volume-adjusted Poisson distributions to cellular autoradiographic grain counts

Radioactive precursor	Labeling condition	Type of distribution fitted	D_{max}[a]	$D_{0.05}$[b]	n[c]
Uracil	Continuous	Normal Poisson[d]	0.1234	0.0789	296
		Volume-adjusted Poisson[e]	0.0757		
Leucine	Continuous (long exposure)	Normal Poisson	0.2194	0.0613	510
		Volume-adjusted Poisson	0.1584		
Leucine	Continuous (short exposure)	Normal Poisson	0.0675	0.0778	305
		Volume-adjusted Poisson	0.0495		
Leucine	Pulse	Normal Poisson	0.1264	0.0978	193
		Volume-adjusted Poisson	0.0950		

[a] D_{max} parameter calculated by the Kolmolgorov-Smirnov procedure (21). This is the maximum deviation of the cumulative experimental distribution from the cumulant distribution for the best-fitting volume-adjusted Poisson.

[b] The predicted maximum value that D_{max} may reach, and the fitted distribution that may be considered indistinguishable at the 5% confidence level from the distribution of counts established experimentally.

[c] Number of cells analyzed.

[d] Poisson distribution (equation 1) fitted to data without adjustments being made for the distribution of cell volumes existent in each population.

[e] Poisson distribution fitted to data which considers the distribution of cell volumes present in each population when each cell size class obeys equation 3.

offered the best fit to the data can also be seen by an examination of Table 1, which shows that in each case the D_{max} parameter is smaller for the volume-adjusted Poisson than for the normal Poisson distribution. Furthermore, the D_{max} parameter is small enough in all cases except for the cells continuously labeled with leucine marked long exposure to be consistent with the volume-adjusted Poisson fitting the data at the 5% confidence level. The failure of cells continuously labeled with leucine marked long exposure to fit the volume-adjusted Poisson is interpreted as largely a statistical problem of populations which have high average grain counts. The grain distribution around cells of this same sample incubated for 39 rather than 83 days in which the average grain count was 3.8 rather than 21.4 per cell was easily fitted with a volume-adjusted Poisson at the 5% confidence level (see the data in Table 1 given for cells continuously labeled with leucine marked short exposure).

Thus, the analysis of the distributions of grain counts shown in Table 1 agrees with the visual impression gained from studying the relationship between average grain counts and cell volume in Fig. 1 that the concentration of RNA and protein appears to be relatively invariant over most of the volume range studied. This would argue against the conclusion of Mitchison (21) that cells change in density during normal growth. However, our findings should be quickly qualified, in that Mitchison was examining living cells, whereas we studied fixed dehydrated cells which are known to decrease in volume and whose densities may differ with regard to cell size in a different manner from that of living cells. Also, the density patterns seen by Mitchison could have been due to variations in cellular components other

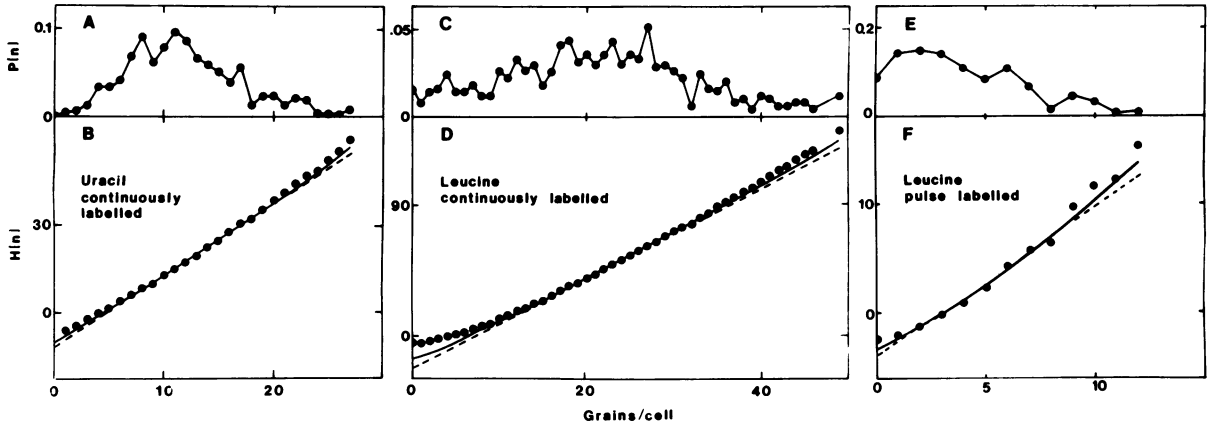

FIG. 2. Analysis of the distribution of autoradiographic grains around whole cells of *S. faecium* which had been continuously labeled with tritiated uracil (A, B) or leucine (C, D) for 12 generations or pulse-labled for 5 min with leucine (E, F) before being fixed. Panels A, C, and E are the frequency distributions of cells [$P(n)$] showing a given number of grains (closed circles). Closed circles in panels B, D, and F are the data in panels A, C, and E transformed by the procedure of Hanawalt et al. (8) (equation 2). Solid lines represent the volume-adjusted Poisson distribution (equation 3) for each population which takes into consideration the distribution of cell volumes. Dashed line represents a simple Poisson distribution (equation 1) which was fitted to the mean grain count for each population.

than RNA or protein or to small variations in RNA and protein concentrations that we would not detect at the 5% confidence level. Finally, while the concentration of RNA and protein might have been relatively invariant in most of our cells, this does not rule out the possibility that the rate of macromolecular synthesis could have been reduced in certain subpopulations of cells, as has been seen in some, but not all, studies of other bacteria (3, 9, 15, 17, 18, 22). For example, for the cells pulse-labeled with leucine in Fig. 2F there were about 4% more cells with zero grains than predicted. To examine this question further, we plotted the number of cells with zero grains as a function of cell volume to determine in cell size terms where these cells with zero grains were located in the population.

Figure 3 shows that the fraction of the population with zero grains decreases smoothly with increasing cell volume (Fig. 3, solid points). However, if the average number of grains in each volume class (m, Fig. 1C) is used to calculate the theoretical fraction of cells that should have zero grains by using a restricted case of equation 1 where $n = 0$ which is $P(0) = e^{-m}$ (Fig. 3, open points), the actual fraction of cells with zero grains is slightly higher than that predicted by $P(0) = e^{-m}$ (except at the extremes of the size range where the sampling error for the calculation of $P(0)$ is large]. These observations suggest that the fraction of metabolically inert cells is very small (14). This would further suggest that the decrease in grain count observed in large and small cells in the pulse-labeled cells shown in Fig. 1C is not a function of a great increase in dead or null-class cells but is likely to be the result of the actual presence of cells with reduced metabolism.

Relationship between initiation of new sites of envelope growth and rate of protein synthesis. As stated, in the past we have shown that a site of envelope growth of *S. faecium* has a limited capacity to increase the volume of a cell (5). At the completion of its synthesis, a site forms two polar caps whose volume shows relatively little variation in size (i.e., the coefficient of variation is ca. 18%). In Fig. 1C it was observed that when the total volume of a cell pulse-labeled with leucine exceeded ca. 0.325 μm^3 the averge grain count decreased. When these data were replotted in Fig. 4 where the average grain count per cell is now presented not as a function of the total cell volume but rather the volume contained by the old growth site in each cell, it can be seen that the average grain count decreases when the old site exceeds ca. 0.12 μm^3. Since the average size of two poles in this population is ca. 0.17 μm^3, the implication is that a site ceases rapid growth when it reaches about 70% of its final capacity (0.12/0.17 μm^3). If 0.12 μm^3 marks the end of the rapid growth phase of a site, one prediction would be that for rapid growth to continue in a cell, new sites must be introduced when old sites approach or exceed this critical size. The cross-hatched region of Fig. 4 shows the frequency of cells with new sites as a function of growth-site volume.

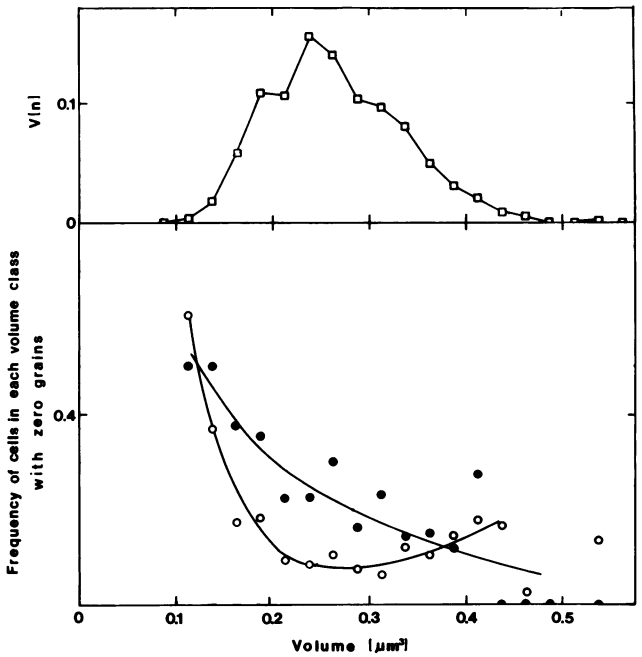

FIG. 3. Comparison of the frequency of cells pulse-labeled with leucine in each volume class with zero grains (closed circles) with the theoretical frequency of cells that should have zero grains (open circles), using the equation $P(0) = e^{-m}$, where m is the average grain count from each volume class taken from Fig. 1C. The open squares indicate the frequency distribution of all cells in the population.

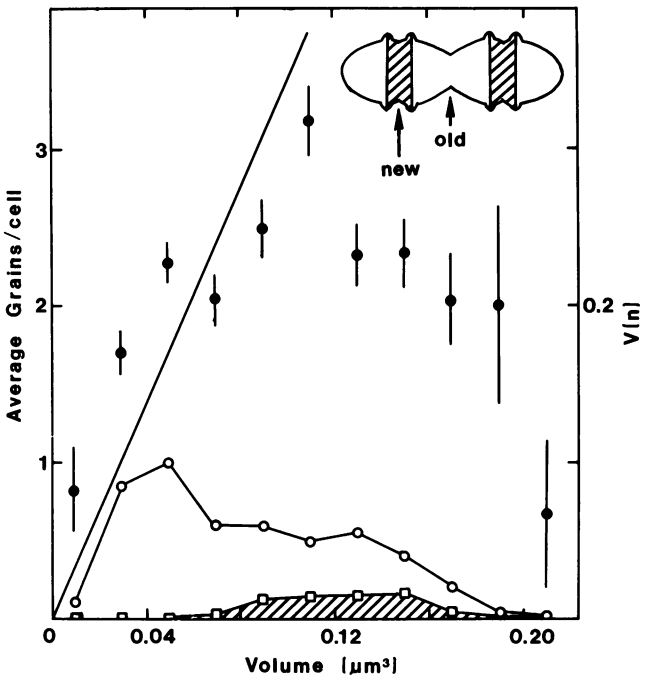

FIG. 4. Relation between average number of autoradiographic grains and the fraction of the total cell volume contained by the old or central envelope growth site (see insert) found in each cell. Each increment of volume equals 0.02 μm^3. The symbols are the same as described in the legend to Fig. 1. Cross-hatched area shows the frequency distribution of cells which have new sites of envelope growth.

Clearly, the appearance of cells with new sites is not precisely regulated in regard to growth-site size or fluctuations in average grain count. Many cells show new sites well before the decrease in grain count is observed, and no saltatory increase in the frequency of cells with new sites is observed after the decrease in grain count is seen at volumes greater than ca. 0.12 μm^3. These data suggest that there is a large variance in regard to growth-site volume (Fig. 4) (or whole-cell volume as well [Fig. 1C]) over which these new sites appear. Furthermore, the introduction of new sites in large cells does not seem to result in an immediate resumption of a rapid rate of protein synthesis in many cells. The average grain count of cells with total volumes >0.2 μm^3 in Fig. 1C with and without new sites was not significantly different (the average was 2.8 and 2.3 grains per cell in each respective group). Possibly a short period is required in some cells after the introduction of new sites before rapid growth is restored. This lag could be a partial explanation for the apparent decrease in the rate of protein synthesis also seen in small cells in Fig. 1C. In this view, the lower grain counts might result from small cells being born with new sites which are still in an initial slow-growth phase. In addition, it has been calculated that about 70% of cells with mass doubling times equivalent to those used here would form new sites just at or shortly after division (16).

Thus, it seems that subpopulations of both large and small cells with reduced metabolism could result from the poor phasing in the introduction of new sites into cells as their old sites reach maximum size limits and possibly from an initial lag in the growth of many new sites after they are made. In addition, our data were inconsistent with the model in which new sites would be made owing to an increase in pressure owing to the cytoplasm growing faster than surface (16, 23, 24). At no point were we able to observe an increase in the rate of protein or the amount of protein or RNA per unit volume in relation to the initiation of new sites of envelope growth.

Technical limitations. The agreement between actual grain distributions of cells labeled with radioactive leucine and uracil and the volume-adjusted Poisson distributions which considered the distribution of cell volumes was in most cases quite good (Fig. 2). As described above, the discrepancies which appeared at low grain counts could have been due in part to subpopulations of cells with reduced metabolism; however, in addition, the deviations noted at both high and low grain counts could also have arisen from several technical problems. These include (i) inadequate correction for coincidence, (ii) improper correction for background; or (iii) variable photographic efficiency in different regions of the autoradiogram.

Coincidence correction. In these experiments, correction for coincidence initially seemed negligible as estimated from the mean projected area in which grains were counted for individual cells (2.5 μm^2) and the mean area of a developed grain (0.0044 μm^2). Thus, if one assumed an even distribution of grains, it would total 2.5/0.0044 = 518 grains to cover a cell. Of course, the coincidence correction would become important at a much lower number of grains per cell. If n grains were observed, then the actual number of grains would be $n/(1 - n/518)$. However, owing to the irregularity in shape of individual grains after development, closely situated and overlapping grains usually could be differentiated from one another in the electron microscope photographs. Consequently, 518 should be replaced by a larger number, perhaps 1,000, since we believed we would count two overlapping grains as two grains, but probably would count three overlapping grains also as two grains.

In all our experiments, the correction for coincidence is negligible. However, detailed measurements showed that grains are not evenly distributed over the counting area; rather, ca. 23% of the observed grains were within 0.07 μm of the cell perimeter. This is to be expected from the geometrical situation of a roughly spherical cell embedded in a sensitive emulsion. Consequently, the more conservative upper grain number which could be counted before coincidence would be total in this band around the cell would be the quotient of the perimeter area ($2.55 \times 0.07 = 0.18$ μm^2) and the average area of a developed grain (0.0044 μm^2). It would only take 41 grains to completely cover this area, or roughly 41/23% = 178 for the whole cell. Multiplying 178 by 2, the correction is the observed count relative to the grain count divided by the factor $1 - n/356$. Therefore, the conservative upper number of grains that could be counted without having more than a 10% loss would be 36, since $1 - 36/356 = 90\%$. In our experiments a few cells were analyzed which had more than 36 grains, but the vast bulk had many fewer. In addition, when the data from this experiment were analyzed by a coincidence correction formula (see Materials and Methods), no significant decrease in D_{max} values was observed.

Background correction. The number of grains outside a 0.5-μm perimeter around the cells was quite small, ranging between 0.09 and 0.188 grains per μm^2. Therefore the background correction is between 0.226 and 0.472 grains for the average-sized cell. When a background subtraction procedure was applied to the data which corrected cell grain counts on the basis of the density of background counts

measured in the particular location in the specimen in which each cell was photographed, the D_{max} values obtained from fitting volume-adjusted Poisson distributions to the corrected data were still significant at the 5% confidence level, but were slightly larger than the uncorrected data (e.g., the D_{max} value for the cells continuously labeled with leucine [short exposure] was 0.0775 after background correction, as contrasted with the value of 0.0495 for cells uncorrected for background grains). The larger D_{max} values were attributed to the difficulties of making accurate background counts when the background counts are as low as observed here and to numerical problems resulting from the need of rounding corrected cell counts so that Poisson distributions could be fit to them. Our conclusion is that the number of background counts in these experiments accounts for little of the difference between the volume-adjusted Poisson and actual distribution of grains around cells.

Variation in photographic efficiency. While background grains and coincidence seem to contribute little to differences between the volume-adjusted Poisson and actual distribution of counts, it would appear that a significant source of technical difficulty was the inherent variation in efficiency which we attribute to a variation in photographic emulsion thickness. This was suggested from an average coefficient of variation of 12% in the average number of grains observed over cells coming from one grid bar opening to another within a single grid.

Conclusions. While in future work we hope to decrease this third technical problem, it would seem that the present data support several conclusions and have certain implications in the development of cell growth models. First, at the 5% confidence level, it seems that the concentration of RNA and protein in most cells remains relatively constant and independent of cell volume. While the concentration of macromolecules does not seem to vary much as cells increase in size, a study of cells pulse-labeled with leucine suggests that there may be a decrease in the rate of synthesis of some cells in the population, especially in large and small cells, and that our data are inconsistent with this apparent decrease in synthesis being the result of a large increased fraction of dead cells in these size ranges.

An analysis of the rate of protein synthesis as a function of the size of envelope growth sites confirmed our previous findings indicating that sites have a finite capacity for growth. It also extends past studies by suggesting that the observed reduction in the rate of protein synthesis occurs when a site reaches about 70% of its maximum final size. It is logical to assume that since each site has a limited capacity for growth, new sites must be initiated in cells with sites that are approaching their maximum sizes for rapid growth to continue or resume. However, it appears that the formation of new sites is not tightly regulated in reference to either increases in growth site or total cell volume, fluctuations in rates of protein synthesis, or changes in the density of RNA or protein. Furthermore, it would seem that the appearance of new sites in cells does not result in an immediate increase in the rate of protein synthesis in all cells. Thus, while it is clear that as a site reaches its maximum size a new site must be introduced into the cell to restore rapid growth, it is not clear why the introduction of new sites is so highly variable in regard to growth sites reaching these critical sizes.

ACKNOWLEDGMENTS

This work was supported by Public Health Service grants AI 10971 from the National Institute of Allergy and Infectious Diseases and GM34222 from the National Institute for General Medicine.

We thank Uwe B. Sleytr for help in developing the autoradiographic techniques, B. D. Monaco for excellent assistance in electron microscopy and digitization, and G. Harvey for preparation of the many versions of the manuscript.

LITERATURE CITED

1. **Caro, L. G.** 1961. Localization of macromolecules in *Escherichia coli*. I. DNA and proteins. J. Biophys. Biochem. Cytol. **9**:539–553.
2. **Caro, L. G., and F. Forro.** 1961. Localization of macromolecules in *Escherichia coli*. II. RNA and its site of synthesis. J. Biophys. Biochem. Cytol. **9**:555–565.
3. **Collins, J. F., and M. H. Richmond.** 1962. Rate of growth of *Bacillus cereus* between divisions. J. Gen. Microbiol. **28**:15–33.
4. **Ecker, R. E., and G. Kokaisl.** 1969. Synthesis of protein, ribonucleic acid, and ribosomes by individual bacterial cells in balanced growth. J. Bacteriol. **98**:1219–1226.
5. **Edelstein, E. M., M. Rosenzweig, L. Daneo-Moore, and M. L. Higgins.** 1980. Unit cell hypothesis for *Streptococcus faecalis*. J. Bacteriol. **143**:499–505.
6. **George, L. A., II, and G. S. Vogt.** 1959. Electron microscopy of autoradiographed radioactive particles. Nature (London) **164**:1474–1475.
7. **Gibson, C. W., L. Daneo-Moore, and M. L. Higgins.** 1983. Initiation of wall assembly sites in *Streptococcus faecium*. J. Bacteriol. **154**:573–579.
8. **Hanawalt, P. C., O. Maaløe, D. J. Cummings, and M. Schaechter.** 1961. The normal DNA replication cycle II. J. Mol. Biol. **3**:156–165.
9. **Harvey, R. J., A. G. Marr, and P. R. Painter.** 1967. Kinetics of growth of individual cells of *Escherichia coli* and *Azotobacter agilis*. J. Bacteriol. **93**:605–617.
10. **Higgins, M. L.** 1976. Three-dimensional reconstruction of whole cells of *Streptococcus faecalis* from thin sections of cells. J. Bacteriol. **127**:1337–1345.
11. **Higgins, M. L., and G. D. Shockman.** 1970. Model for cell wall growth of *Streptococcus faecalis*. J. Bacteriol. **101**:643–648.
12. **Higgins, M. L., and G. D. Shockman.** 1976. Study of a cycle of cell wall assembly in *Streptococcus faecalis* by three dimensional reconstructions of thin sections of cells. J. Bacteriol. **127**:1346–1358.
13. **Hinks, R. P., L. Daneo-Moore, and G. D. Shockman.** 1976. Cellular autolytic activity in synchronized populations of *Streptococcus faecium*. J. Bacteriol. **133**:822–829.
14. **Koch, A. L.** 1980. Does the variability of the cell cycle result from one or many chance events? Nature (London) **286**:80–82.
15. **Koch, A. L.** 1977. Does the initiation of chromosome replication regulate cell division? Adv. Microb. Physiol. **16**:49–97.
16. **Koch, A. L., and M. L. Higgins.** 1984. Control of wall band splitting in *Streptococcus faecalis*. J. Gen. Microbiol. **130**:735–745.
17. **Koppes, L. J. H., N. Overbeeke, and N. Nanninga.** 1978. DNA replication pattern and cell wall growth in *Escherichia coli* PAT84. J. Bacteriol. **133**:1053–1061.
18. **Koppes, L. J. H., C. L. Woldringh, and N. Nanninga.** 1978. Size variations and correlation of different cell cycle events in slow-growing *Escherichia coli*. J. Bacteriol. **134**:423–433.
19. **Kowpriwa, B.** 1973. A reliable, standardized method for ultrastructural electron microscopic radioautography. Histochemie **37**:1–17.
20. **Kowpriwa, B. M.** 1975. A comparison of various procedures for fine grain development in electron microscopic radioautography. Histochemie **44**:201–224.
21. **Mitchison, J. M.** 1961. The growth of single cells. III. *Streptococcus faecalis*. Exp. Cell Res. **22**:208–225.
22. **Nanninga, N., and C. L. Woldringh.** 1985. Cell growth, genome duplication and cell division, p. 259–318. *In* N. Nanninga (ed.), Molecular cytology of *Escherichia coli*. Academic Press, Inc., New York.
23. **Previc, E. P.** 1970. Biochemical determination of bacterial morphology and the geometry of cell division. J. Theor. Biol. **27**:471–497.
24. **Prichard, R. H.** 1974. On the growth and form of a bacterial cell.

Philos. Trans. R. Soc. London Ser. B **207**:303–336.
25. **Shockman, G. D.** 1962. Amino acids, p. 567–673. *In* F. Kavanagh (ed.), Analytical microbiology. Academic Press, Inc., New York.
26. **Siegel, S.** 1956. Nonparametric statistics for the behavioural sciences. McGraw-Hill Book Co., New York.
27. **Toennies, G., L. Iszard, N. B. Rogers, and G. D. Shockman.** 1961. Cell multiplication studied with an electronic particle counter. J. Bacteriol. **82**:857–866.
28. **Toennies, G., and G. D. Shockman.** 1958. Growth chemistry of *Streptococcus faecalis*. Proc. Int. Congr. Biochem. **13**:365–394.
29. **Van Tubergen, R. P., and R. B. Setlow.** 1961. Quantitative radioautographic studies on exponentially growing cultures of *Escherichia coli*. The distribution of parental DNA, RNA, protein and cell wall among progeny cells. Biophys. J. **1**:589–625.